Lithuanian Journal of Physics, Vol. **57**, No. 2, pp. 78–87 (2017)

THE CRYSTALLINE STRUCTURE OF $SrRuO_3$: APPLICATION OF HYBRID SCHEME TO THE DENSITY FUNCTIONALS REVISED FOR SOLIDS

Š. Masys and V. Jonauskas

Institute of Theoretical Physics and Astronomy, Vilnius University, Saulėtekio 3, LT-10257 Vilnius, Lithuania
E-mail: sarunas.masys@tfai.vu.lt

Received 23 December 2016; accepted 16 March 2017

The crystalline structure of ground-state orthorhombic $SrRuO_3$ is reproduced by applying the hybrid density functional theory scheme to the functionals based on the revised generalized-gradient approximations for solid-state calculations. The amount of Hartree–Fock (HF) exchange energy is varied in the range of 5–20% in order to systematically ascertain the optimum value of HF mixing which in turn ensures the best correspondence to the experimental measurements. Such investigation allows one to expand the set of tools that could be used for the efficient theoretical modelling of, for example, only recently stabilized phases of $SrRuO_3$, helping to resolve issues emerging for the experimentalists.

Keywords: Perovskite crystals, density functional theory, crystalline structure

PACS: 71.15.Mb, 71.15.Nc, 61.50.-f

1. Introduction

Strontium ruthenate $SrRuO_3$ is a perovskite-structured conductive ferromagnet which upon heating undergoes a series of phase transformations: orthorhombic (*Pbnm*) $\xrightarrow{820\text{K}}$ tetragonal (*I*4/*mcm*) $\xrightarrow{950\text{K}}$ cubic ($Pm\bar{3}m$) [1]. Nowadays $SrRuO_3$ fascinates researchers because of its pivotal role of being a key integrant for fabrication of oxide heterostructures and superlattices, which in turn have the potential to contribute to new functionalities in electronics and spintronics [2]. However, by looking back from a 50-year perspective one can find some 1,000 papers spanning the physics, materials science, and applications of $SrRuO_3$ in its bulk and thin-film form, and notice the fact that interest in this material continuously increases.

A recent observation that pairwise differences between the results of modern solid-state codes, based on the density functional theory (DFT) approaches, are comparable to those between different high-precision experiments [3] sheds a new light on the predictive potential of the first-principles simulations. In our previous paper [4], we have carefully benchmarked a bunch of DFT functionals – including local density approximation, generalized-gradient approximations (GGAs), and hybrids – in order to identify the ones that are the best at reproducing the crystalline structure of ground-state orthorhombic $SrRuO_3$. The importance of such calculations has recently grown to a new level due to the experimental breakthrough in stabilizing tetragonal and monoclinic phases of $SrRuO_3$ at room temperature – the lack of the precision while determining the exact space-group symmetry for these stabilized systems [5] paves the way to exploit the predictive power of DFT simulations. But in order to

take advantage of it, firstly one has to be aware of the functionals that could potentially lead to precise reproduction of various crystalline structures of $SrRuO_3$. Our observations, based on the direct comparison to the low-temperature experimental data of orthorhombic symmetry, indicate that a hybrid scheme combined with the GGAs revised for solids is the most appropriate tool for the accurate description of the external (lattice constants and volume) and internal (tilting and rotation angles together with internal angles and bond distances of RuO_6 octahedra) structural parameters simultaneously. However, the amount of Hartree–Fock (HF) exchange energy smaller than the standard 25% should be preferred, most likely 16% as in B1WC [6] or so. Having said that, we find it important to extend our previous study by investigating the influence of HF exchange in the range of 5–20% and thus to determine in a *systematic* fashion the best option for $SrRuO_3$. What is more, our goal is to include all three revised GGAs for solids, namely, PBEsol [7], SOGGA [8], and WC [9], instead of focusing on a single one of them. By doing so, we expand the suitable set of tools for the efficient theoretical modelling of $SrRuO_3$ and also demonstrate how it can be employed to clarify the issues raised by researchers in the laboratory, like in the work of Vailionis et al. [5].

2. Computational details

In this work, the ferromagnetic phases of $SrRuO_3$ were simulated using the CRYSTAL14 code [10] which employs a linear combination of atom-centered Gaussian orbitals. The small-core Hay–Wadt pseudopotentials [11] were utilized to describe the inner-shell electrons ($1s^2 2s^2 2p^6 3s^2 3p^6 3d^{10}$) of Sr and Ru atoms. The valence part of the basis set for Sr ($4s^2 4p^6 5s^2$) was taken from the $SrTiO_3$ study [12], while the valence functions for Ru ($4s^2 4p^6 4d^7 5s^1$) were adopted from our previous work on non-stoichiometric $SrRuO_3$ [13]. Concerning the oxygen atom, all-electron basis set was applied from the calcium carbonate study [14].

The default values were chosen for most of the technical setup while performing a full and constrained geometry optimization – the details can be found in the CRYSTAL14 user's manual [15]. However, in terms of atomic units, a parameter that defines the convergence threshold on total energy and five parameters that define the truncation criteria for bielectronic integrals were tightened to 10^{-8} and 10^{-8}, 10^{-8}, 10^{-8}, 10^{-8}, and 10^{-16}, respectively. Truncation was made according to the overlap-like criteria: when the overlap between two atomic orbitals was smaller than 10^{-x}, the corresponding integral was disregarded or evaluated in a less precise way. The allowed root-mean-square values of energy gradients and nuclear displacements were correspondingly set to $6{\cdot}10^{-5}$ and $1.2{\cdot}10^{-4}$. In order to improve the self-consistence field convergence, the Kohn–Sham matrix mixing technique (at 80%) together with the Anderson's method [16], as proposed by Hamman [17], were applied. The reciprocal-space integration was performed with shrinking factors of 10 for *I*4/*mmm* and 8 for *Pbnm* and *Cmcm* symmetries that resulted in 102, 125, and 105 independent **k** points in the first irreducible Brillouin zone, respectively.

Within the employed hybrid scheme, the exchange–correlation energy may be given in the form

$$E_{XC}^{Hybrid} = aE_X^{HF} + (1-a)\,E_X^{GGA} + E_C^{PBE}, \quad (1)$$

where E_X^{GGA} stands for the exchange energy of PBEsol, SOGGA, or WC approaches, whereas E_C^{PBE} represents the correlation part of PBE functional [18]. The mixing parameter a that controls the amount of HF exchange energy E_X^{HF} was varied from 0.05 to 0.2.

3. Results and discussion

3.1. Benchmark of hybrid scheme

The geometry of ground-state orthorhombic (*Pbnm*) $SrRuO_3$ is depicted in Fig. 1. The equilibrium structural parameters calculated using PBEsol, SOGGA, and WC functionals are given in corresponding Tables 1, 2 and 3. The mean absolute relative errors (MAREs) were evaluated according to the expression

$$\mathrm{MARE} = \frac{100}{n}\sum_{i=1}^{n}\left|\frac{p_i^{Calc.} - p_i^{Expt.}}{p_i^{Expt.}}\right|, \quad (2)$$

in which $p_i^{Calc.}$ and $p_i^{Expt.}$ are the calculated and experimental values of the considered parameter, respectively. A visual representation of MAREs dependence on the percentage of HF mixing can be

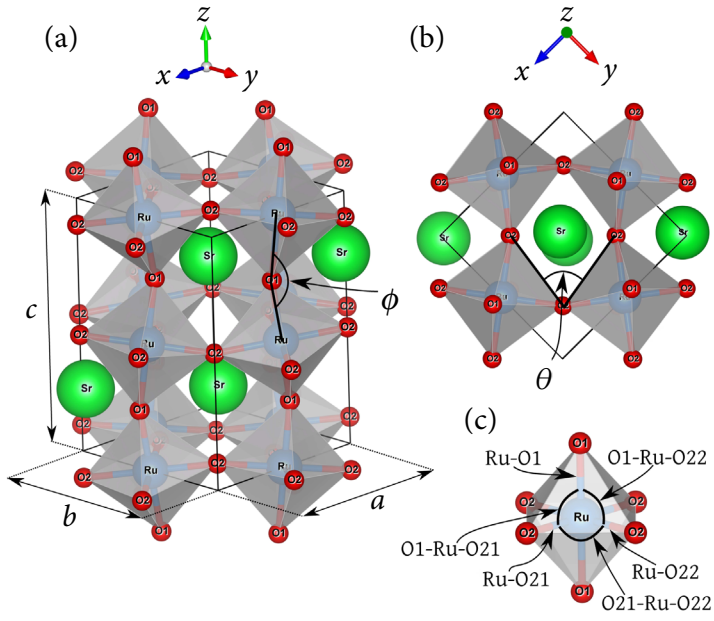

Fig. 1. Schematic representation of (a) the crystalline structure of $SrRuO_3$, (b) its top view, and (c) octahedral parameters. Notations O1 and O2 label oxygen atoms at the apical and planar positions of the RuO_6 octahedra, respectively. The drawings, as well as in Fig. 3, were produced with the visualization program VESTA [22].

Table 1. Structural parameters of *Pbnm* $SrRuO_3$ calculated within the PBEsol framework and compared to the experimental data. Lattice constants a, b, and c together with bond distances Ru-O1, Ru-O21, and Ru-O22 are given in Å, volume V is given in Å^3, angles ϕ, θ, O1-Ru-O21, O1-Ru-O22, and O21-Ru-O22 are given in degrees. MARE (in %) stands for the mean absolute relative error: $MARE_1$ is evaluated for a, b, c and V; $MARE_2$ for ϕ and θ; $MARE_3$ for Ru-O1, Ru-O21, Ru-O22, O1-Ru-O21, O1-Ru-O22, and O21-Ru-O22; $MARE_T$ denotes the total MARE of all 12 structural parameters. The numbers in brackets (in %) represent absolute relative errors for each structural parameter.

	PBEsol	PBEsol with percentage of HF mixing				Expt.
		5%	10%	15%	20%	
a	5.568	5.563	5.555	5.545	5.534	5.566
	(0.05)	(0.04)	(0.19)	(0.38)	(0.56)	
b	5.538	5.523	5.513	5.504	5.518	5.531
	(0.13)	(0.12)	(0.32)	(0.48)	(0.22)	
c	7.858	7.845	7.831	7.821	7.801	7.844
	(0.18)	(0.01)	(0.16)	(0.29)	(0.55)	
V	242.30	241.08	239.83	238.68	238.22	241.44
	(0.36)	(0.15)	(0.67)	(1.14)	(1.33)	
ϕ	159.98	160.31	160.85	161.51	160.35	161.97
	(1.23)	(1.02)	(0.69)	(0.28)	(1.00)	
θ	74.43	75.31	75.83	76.19	76.04	77.16
	(3.54)	(2.40)	(1.72)	(1.25)	(1.45)	
Ru-O1	1.995	1.991	1.986	1.981	1.979	1.986
	(0.46)	(0.25)	(0.01)	(0.23)	(0.32)	
Ru-O21	1.999	1.993	1.988	1.982	1.992	1.986
	(0.63)	(0.33)	(0.05)	(0.22)	(0.29)	
Ru-O22	1.997	1.991	1.986	1.981	1.973	1.987
	(0.50)	(0.21)	(0.07)	(0.33)	(0.72)	
O1-Ru-O21	90.20	90.19	90.19	90.19	90.52	90.25
	(0.06)	(0.07)	(0.07)	(0.07)	(0.30)	
O1-Ru-O22	90.38	90.45	90.46	90.45	90.05	90.31
	(0.07)	(0.15)	(0.16)	(0.15)	(0.30)	
O21-Ru-O22	91.21	91.28	91.26	91.20	90.88	91.08
	(0.14)	(0.22)	(0.20)	(0.12)	(0.22)	

Table 1 (continued)

	PBEsol	PBEsol with percentage of HF mixing				Expt.
		5%	10%	15%	20%	
$MARE_1$	0.18	0.08	0.33	0.57	0.67	
$MARE_2$	2.38	1.71	1.21	0.76	1.22	
$MARE_3$	0.31	0.20	0.09	0.19	0.36	
$MARE_T$	0.61	0.41	0.36	0.41	0.61	

Table 2. Structural parameters of *Pbnm* $SrRuO_3$ calculated within the SOGGA framework and compared to the experimental data. Lattice constants *a*, *b*, and *c* together with bond distances Ru-O1, Ru-O21, and Ru-O22 are given in Å, volume *V* is given in Å^3, angles ϕ, θ, O1-Ru-O21, O1-Ru-O22, and O21-Ru-O22 are given in degrees. MARE (in %) stands for the mean absolute relative error: $MARE_1$ is evaluated for *a*, *b*, *c*, and *V*; $MARE_2$ for ϕ and θ; $MARE_3$ for Ru-O1, Ru-O21, Ru-O22, O1-Ru-O21, O1-Ru-O22, and O21-Ru-O22; $MARE_T$ denotes the total MARE of all 12 structural parameters. The numbers in brackets (in %) represent absolute relative errors for each structural parameter.

	SOGGA	SOGGA with percentage of HF mixing				Expt.
		5%	10%	15%	20%	
a	5.565	5.561	5.553	5.542	5.532	5.566
	(0.00)	(0.08)	(0.22)	(0.42)	(0.59)	
b	5.534	5.520	5.510	5.502	5.496	5.531
	(0.07)	(0.19)	(0.37)	(0.52)	(0.62)	
c	7.854	7.841	7.827	7.818	7.820	7.844
	(0.12)	(0.04)	(0.21)	(0.34)	(0.30)	
V	241.90	240.71	239.48	238.37	237.78	241.44
	(0.19)	(0.30)	(0.81)	(1.27)	(1.52)	
ϕ	159.97	160.30	160.79	161.46	160.79	161.97
	(1.23)	(1.03)	(0.73)	(0.31)	(0.73)	
θ	74.40	75.30	75.90	76.25	76.80	77.16
	(3.57)	(2.41)	(1.63)	(1.18)	(0.46)	
Ru-O1	1.994	1.990	1.985	1.980	1.983	1.986
	(0.41)	(0.20)	(0.05)	(0.27)	0.14)	
Ru-O21	1.998	1.992	1.987	1.981	1.993	1.986
	(0.58)	(0.28)	(0.01)	(0.26)	(0.33)	
Ru-O22	1.996	1.990	1.985	1.980	1.960	1.987
	(0.44)	(0.16)	(0.11)	(0.38)	(1.37)	
O1-Ru-O21	90.21	90.21	90.19	90.20	90.25	90.25
	(0.05)	(0.05)	(0.06)	(0.06)	(0.00)	
O1-Ru-O22	90.39	90.46	90.46	90.45	90.00	90.31
	(0.08)	(0.17)	(0.16)	(0.15)	(0.35)	
O21-Ru-O22	91.21	91.30	91.28	91.20	91.05	91.08
	(0.14)	(0.24)	(0.22)	(0.13)	(0.04)	
$MARE_1$	0.10	0.15	0.41	0.64	0.76	
$MARE_2$	2.40	1.72	1.18	0.75	0.59	
$MARE_3$	0.29	0.18	0.10	0.21	0.37	
$MARE_T$	0.57	0.43	0.38	0.44	0.54	

Table 3. Structural parameters of *Pbnm* $SrRuO_3$ calculated within the WC framework and compared to the experimental data. Lattice constants *a*, *b*, and *c* together with bond distances Ru-O1, Ru-O21, and Ru-O22 are given in Å, volume *V* is given in Å^3, angles ϕ, θ, O1-Ru-O21, O1-Ru-O22, and O21-Ru-O22 are given in degrees. MARE (in %) stands for the mean absolute relative error: $MARE_1$ is evaluated for *a*, *b*, *c*, and *V*; $MARE_2$ for ϕ and θ; $MARE_3$ for Ru-O1, Ru-O21, Ru-O22, O1-Ru-O21, O1-Ru-O22, and O21-Ru-O22; $MARE_T$ denotes the total MARE of all 12 structural parameters. The numbers in brackets (in %) represent absolute relative errors for each structural parameter.

	WC	WC with percentage of HF mixing				Expt.
		5%	10%	15%	20%	
a	5.580	5.573	5.565	5.556	5.543	5.566
	(0.26)	(0.14)	(0.01)	(0.18)	(0.40)	
b	5.553	5.538	5.526	5.515	5.531	5.531
	(0.40)	(0.14)	(0.08)	(0.28)	(0.02)	
c	7.877	7.862	7.847	7.834	7.813	7.844
	(0.42)	(0.23)	(0.04)	(0.12)	(0.40)	
V	244.08	242.69	241.32	240.05	239.57	241.44
	(1.09)	(0.52)	(0.05)	(0.58)	(0.78)	
ϕ	159.58	160.03	160.55	161.15	159.98	161.97
	(1.47)	(1.20)	(0.87)	(0.51)	(1.23)	
θ	74.21	75.01	75.59	76.08	75.93	77.16
	(3.82)	(2.79)	(2.03)	(1.40)	(1.60)	
Ru-O1	2.001	1.996	1.990	1.985	1.983	1.986
	(0.77)	(0.51)	(0.24)	(0.02)	(0.11)	
Ru-O21	2.005	1.999	1.993	1.987	1.998	1.986
	(0.95)	(0.62)	(0.32)	(0.04)	(0.59)	
Ru-O22	2.003	1.997	1.991	1.985	1.976	1.987
	(0.80)	(0.48)	(0.19)	(0.10)	(0.54)	
O1-Ru-O21	90.14	90.14	90.14	90.14	90.42	90.25
	(0.12)	(0.12)	(0.12)	(0.12)	(0.19)	
O1-Ru-O22	90.33	90.39	90.39	90.38	89.90	90.31
	(0.02)	(0.08)	(0.09)	(0.08)	(0.46)	
O21-Ru-O22	91.21	91.26	91.25	91.22	90.86	91.08
	(0.14)	(0.19)	(0.19)	(0.15)	(0.24)	
$MARE_1$	0.55	0.26	0.05	0.29	0.40	
$MARE_2$	2.65	1.99	1.45	0.95	1.41	
$MARE_3$	0.47	0.34	0.19	0.08	0.36	
$MARE_T$	0.86	0.59	0.35	0.30	0.55	

found in Fig. 2. For the sake of accuracy, the low-temperature experimental data, also presented in Tables 1 and 2, were taken as an arithmetic average of the results obtained from the 1.5 K [19] and 10 K [20] neutron diffraction measurements. It should also be mentioned that no zero-point anharmonic expansion (ZPAE) corrections to the experimental data were applied, since our previous non-magnetic calculations [21] indicate that the ZPAE correction for the lattice constant of cubic $SrRuO_3$ reaches at most ~0.13% and therefore can be treated as negligible.

An analysis of Fig. 2(a) reveals that the performance of SOGGA functional in reproducing lattice constants and volume is already optimum and the addition of HF exchange only worsens

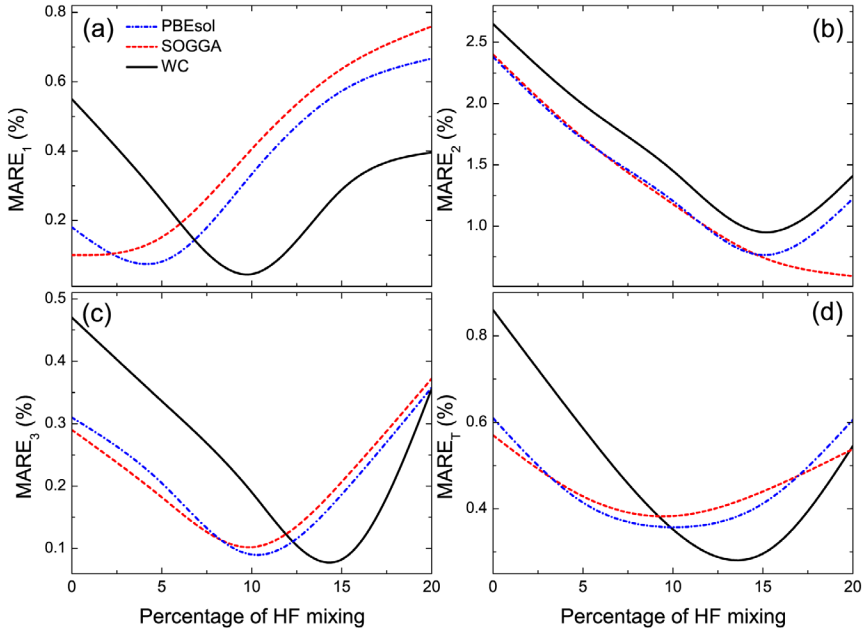

Fig. 2. Influence of the amount of HF mixing on (a) $MARE_1$, (b) $MARE_2$, (c) $MARE_3$, and (d) $MARE_T$. The presented curves were smoothed by using a cubic spline interpolation.

the results. However, a small amount (~5%) of E_X^{HF} appears to be favourable for the PBEsol approach which shows a slight improvement in $MARE_1$ reducing it from 0.18 to 0.08%. A more pronounced amelioration can be noticed for the WC functional, since its $MARE_1$ decreases from 0.55 to 0.05% at 10% of HF mixing. On the whole, in the range of a = 0–0.1 all three revised GGAs are able to yield $MARE_1$ values of 0.1% or even less, and it can be considered as a truly impressive result. But despite that, a completely different trend is observed in Fig. 2(b) where the tilting and rotation angles of RuO_6 octahedra are taken into account. One can note that here at least ~15% of HF mixing is necessary for WC and slightly less for PBEsol and SOGGA in order to get below the so-called satisfactory threshold of MAREs set to 1% in our previous paper [4]. The higher $MARE_2$ values compared to the errors of lattice constants and volume may be explained by the fact that variations in tilting and rotation angles involve very subtle energy changes which are much more harder to deal with. A somewhat different behaviour of the SOGGA functional in comparison to those of PBEsol and WC at 20% of HF exchange allows the decrease of $MARE_2$ to 0.59% showing that the range of a = 0.15–0.2 seems to be the most appropriate choice for the tilting and rotation angles. This observation is perfectly consistent with the result of mB1WC [4] – a combination of WC exchange, PBE correlation, and 16% of HF mixing – which is a bit lower (0.84%) compared to the $MARE_2$ value of WC at 15% of HF exchange (0.95%). But amounts of E_X^{HF} larger than 20% should not lead to a further improvement though, at least for PBEsol and WC approximations.

Similarly to lattice constants and volume, bond distances and bond angles of RuO_6 octahedra are also reproduced with a satisfactory accuracy using a pure GGA scheme. From Fig. 2(c) and Tables 1–3 one can note that PBEsol, SOGGA, and WC functionals alone achieve $MARE_3$ <0.5%, however, additional 10% of HF mixing for PBEsol and SOGGA and 15% for WC allow the improvement of $MARE_3$ values to 0.09%, 0.1%, and 0.08%, respectively. Therefore, it becomes obvious that the range of a = 0.1–0.15 is a priority option for the most accurate description of RuO_6 geometry. Interestingly, the same tendency also holds for the overall performance of the functionals represented by variation of $MARE_T$ in Fig. 2(d). Here, the $MARE_T$ value of WC drops from 0.86 to 0.3% as the amount of HF exchange is increased up to 15%, while for the PBEsol and SOGGA approaches the improvement is not that impressive but still noticeable – from 0.61 to 0.36% for the former and from 0.57 to 0.38% for the latter at 10% of HF mixing. These findings clearly indicate that the hybrid scheme has a positive impact on the overall results of all three considered functionals, most likely due to the reduction of the self-interaction error which stems from the fact that electrons are allowed to spuriously interact with themselves

within the GGA framework. An optimum value of the HF mixing parameter *a* falls in the range of 0.1–0.15, and it is definitely smaller than the typical one of 0.25 usually applied in the first-principles calculations.

3.2. Employment for tensile strained $SrRuO_3$

In the study of Vailionis et al. [5], the authors investigate the lattice response to the compressive and tensile strains in $SrRuO_3$ thin films grown on different substrates. Under compressive strain, the $SrRuO_3$ thin film possesses a monoclinic $P2_1/m$ lattice, but under tensile strain, the situation is not that straightforward – subtle differences between pseudotetragonal *Cmcm* and tetragonal *I*4/*mmm* lattices, shown in Fig. 3, are too small to be detected experimentally. From a theoretical point of view, this issue could be resolved by selecting the most appropriate DFT approximation and performing geometry optimization for both systems. Therefore, among our tested PBEsol, SOGGA, and WC approaches we choose the PBEsol functional and combine it with 10% of HF mixing. Although a combination of WC with 15% of HF exchange exhibits a slightly better overall performance, PBEsol is a more common choice for the plane-wave calculations with open-source pseudopotential libraries, making it easier to reproduce our findings. The results of full geometry optimization, given in Table 4, indicate

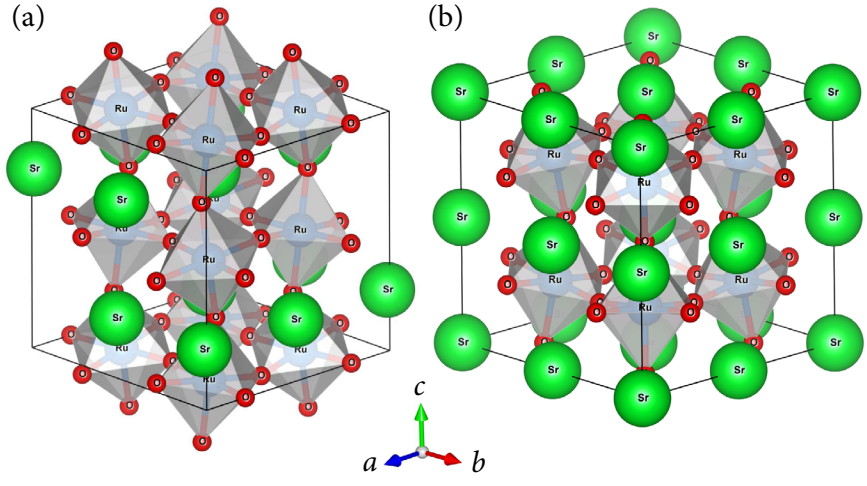

Fig. 3. The crystalline structure of (a) *Cmcm* and (b) *I*4/*mmm* symmetries of $SrRuO_3$.

Table 4. Fractional coordinates, lattice constants (in Å), and total energy penalty (in meV per formula unit) for the fully relaxed *Cmcm* and *I*4/*mmm* symmetries of $SrRuO_3$ calculated by combining PBEsol functional with 10% of HF mixing. ΔE is evaluated with respect to the total energy of ground-state (*Pbnm*) $SrRuO_3$.

	Cmcm				*I*4/*mmm*			
	Wyckoff position	*x*	*y*	*z*	Wyckoff position	*x*	*y*	*z*
Sr	4*c*	0.0	–0.0121	0.25	2*a*	0.0	0.0	0.0
Sr	4*c*	0.0	0.4879	0.25	2*b*	0.0	0.0	–0.5
Sr	–	–	–	–	4*c*	0.0	–0.5	0.0
Ru	8*d*	0.25	0.25	0.0	8*f*	0.25	0.25	0.25
O	8*e*	0.2141	0.0	0.0	8*h*	0.2205	0.2205	0.0
O	8*f*	0.0	0.2841	–0.4648	16*n*	0.0	0.2519	0.2829
O	8*g*	–0.2128	0.2487	0.25	–	–	–	–
a		7.776				7.858		
b		7.852				7.858		
c		7.858				7.793		
ΔE		19.3				55.1		

Table 5. Fractional coordinates and total energy penalty (in meV per formula unit) for the internally relaxed *Cmcm* and *I*4/*mmm* symmetries of $SrRuO_3$ calculated by combining PBEsol functional with 10% of HF mixing. Lattice constants (in Å) are fixed to the values that correspond to the experimental measurements [5]. ΔE is evaluated with respect to the total energy of ground-state (*Pbnm*) $SrRuO_3$.

	Cmcm				*I*4/*mmm*			
	Wyckoff position	*x*	*y*	*z*	Wyckoff position	*x*	*y*	*z*
Sr	4*c*	0.0	–0.0115	0.25	2*a*	0.0	0.0	0.0
Sr	4*c*	0.0	0.4877	0.25	2*b*	0.0	0.0	–0.5
Sr	–	–	–	–	4*c*	0.0	–0.5	0.0
Ru	8*d*	0.25	0.25	0.0	8*f*	0.25	0.25	0.25
O	8*e*	0.2123	0.0	0.0	8*h*	0.2214	0.2214	0.0
O	8*f*	0.0	0.2847	–0.4679	16*n*	0.0	0.2518	0.2824
O	8*g*	–0.2157	0.2498	0.25	–	–	–	–
a		7.897				7.897		
b		7.829				7.897		
c		7.903				7.903		
ΔE		36.1				76.2		

that the *Cmcm* is energetically more favourable than the *I*4/*mmm* symmetry, since its total energy penalty evaluated with respect to the ground-state $SrRuO_3$ is ~36 meV per formula unit lower. However, fully relaxed structures may not necessarily reflect tendencies present in strained systems. For this reason, we have also carried out constrained geometry optimization with structural parameters fixed to the experimentally measured ones [5]. For the *I*4/*mmm* symmetry, lattice constants were set by applying the requirement that *a* and *c*, which in turn are fully clamped by the $DyScO_3$ substrate in the $SrRuO_3$ thin film, have to be equal to those of the *Cmcm* symmetry. The obtained results, presented in Table 5, imply that under weak tensile strain $SrRuO_3$ indeed prefers the *Cmcm* rather than the *I*4/*mmm* lattice, as the difference in total energy penalty is ~40 meV per formula unit in favour of the former symmetry. This finding allows to conclusively dispel the uncertainty the experimentalists have previously dealt with.

4. Conclusions

In this study, we have *systematically* investigated the influence of 5–20% of HF exchange on the performance of revised GGAs for solids – PBEsol, SOGGA, and WC – in reproducing the crystalline structure of ground-state orthorhombic (*Pbnm*) $SrRuO_3$. The structural parameters of the system were distinguished into three categories: (a) lattice constants and volume, (b) tilting and rotation angles of RuO_6 octahedra, and (c) internal angles and bond distances within RuO_6 octahedra. The obtained results indicate that optimum amounts of HF mixing, which ensure the smallest deviations from the experimental measurements, for the corresponding categories fall in the range of (a) 0–10%, (b) 15–20%, and (c) 10–15%. The overall performance of the tested functionals in reproducing structural parameters in all three categories yields deviations smaller than 0.4%, namely, 0.3% for WC at 15% of HF exchange and 0.36% for PBEsol with 0.38% for SOGGA at 10% of HF mixing. Thus, in the case of the full reproduction of $SrRuO_3$ geometry, 10–15% of HF exchange can be considered as the recommended amount for the revised GGA frameworks. These findings expand the available set of tools for theoretical simulations of $SrRuO_3$ by revealing that the PBEsol and SOGGA approaches can also be combined with the HF exchange as efficiently as our previously studied mB1WC scheme based on the WC approximation. An application of PBEsol with 10% of HF mixing to the geometry of tensile strained $SrRuO_3$ implies that the system apparently favours the *Cmcm* over the *I*4/*mmm* space-group symmetry, resolving the issue previously raised by the researchers investigating $SrRuO_3$ thin films.

The authors are thankful for the high-performance computing resources provided by the IT Open Access Centre of Vilnius University.

References

[1] B.J. Kennedy and B.A. Hunter, High-temperature phases of $SrRuO_3$, Phys. Rev. B **58**, 653 (1998).

[2] G. Koster, L. Klein, W. Siemons, G. Rijnders, J.S. Dodge, C.-B. Eom, D.H.A. Blank, and M.R. Beasley, Structure, physical properties, and applications of $SrRuO_3$ thin films, Rev. Mod. Phys. **84**, 253 (2012).

[3] K. Lejaeghere, G. Bihlmayer, T. Björkman, P. Blaha, S. Blügel, V. Blum, D. Caliste, I.E. Castelli, S.J. Clark, A. Dal Corso, et al., Reproducibility in density functional theory calculations of solids, Science **351**, aad3000 (2016).

[4] Š. Masys and V. Jonauskas, On the crystalline structure of orthorhombic $SrRuO_3$: A benchmark study of DFT functionals, Comput. Mater. Sci. **124**, 78 (2016).

[5] A. Vailionis, H. Boschker, W. Siemons, E.P. Houwman, D.H.A. Blank, G. Rijnders, and G. Koster, Misfit strain accommodation in epitaxial ABO_3 perovskites: Lattice rotations and lattice modulations, Phys. Rev. B **83**, 064101 (2011).

[6] D.I. Bilc, R. Orlando, R. Shaltaf, G.-M. Rignanese, J. Íñiguez, and P. Ghosez, Hybrid exchange-correlation functional for accurate prediction of the electronic and structural properties of ferroelectric oxides, Phys. Rev. B **77**, 165107 (2008).

[7] J.P. Perdew, A. Ruzsinszky, G.I. Csonka, O.A. Vydrov, G.E. Scuseria, L.A. Constantin, X. Zhou, and K. Burke, Restoring the density-gradient expansion for exchange in solids and surfaces, Phys. Rev. Lett. **100**, 136406 (2008).

[8] Y. Zhao and D.G. Truhlar, Construction of a generalized gradient approximation by restoring the density-gradient expansion and enforcing a tight Lieb–Oxford bound, J. Chem. Phys. **128**, 184109 (2008).

[9] Z. Wu and R.E. Cohen, More accurate generalized gradient approximation for solids, Phys. Rev. B **73**, 235116 (2006).

[10] R. Dovesi, R. Orlando, A. Erba, C.M. Zicovich-Wilson, B. Civalleri, S. Casassa, L. Maschio, M. Ferrabone, M. De La Pierre, P. D'Arco, et al., CRYSTAL14: A program for the *ab initio* investigation of crystalline solids, Int. J. Quantum Chem. **114**, 1287 (2014).

[11] P.J. Hay and W.R. Wadt, *Ab initio* effective core potentials for molecular calculations. Potentials for K to Au including the outermost core orbitals, J. Chem. Phys. **82**, 299 (1985).

[12] S. Piskunov, E. Heifets, R. Eglitis, and G. Borstel, Bulk properties and electronic structure of $SrTiO_3$, $BaTiO_3$, $PbTiO_3$ perovskites: an *ab initio* HF/DFT study, Comput. Mater. Sci. **29**, 165 (2004).

[13] Š. Masys, V. Jonauskas, S. Grebinskij, S. Mickevičius, V. Pakštas, and M. Senulis, Theoretical and experimental study of non-stoichiometric $SrRuO_3$: a role of oxygen vacancies in electron correlation effects, Lith. J. Phys. **53**, 150 (2013).

[14] L. Valenzano, F.J. Torres, D. Klaus, F. Pascale, C.M. Zicovich-Wilson, and R. Dovesi, *Ab initio* study of the vibrational spectrum and related properties of crystalline compounds; the case of $CaCO_3$ calcite, Z. Phys. Chem. **220**, 893 (2006).

[15] R. Dovesi, V.R. Saunders, C. Roetti, R. Orlando, C.M. Zicovich-Wilson, F. Pascale, B. Civalleri, K. Doll, N.M. Harrison, I.J. Bush, et al., *CRYSTAL14 User's Manual* (University of Torino, Torino, 2014).

[16] D.G. Anderson, Iterative procedures for nonlinear integral equations, J. Assoc. Comput. Mach. **12**, 547 (1965).

[17] D.R. Hamann, Semiconductor charge densities with hard-core and soft-core pseudopotentials, Phys. Rev. Lett. **42**, 662 (1979).

[18] J.P. Perdew, K. Burke, and M. Ernzerhof, Generalized gradient approximation made simple, Phys. Rev. Lett. **77**, 3865 (1996).

[19] S.N. Bushmeleva, V.Y. Pomjakushin, E.V. Pomjakushina, D.V. Sheptyakov, and A.M. Balagurov, Evidence for the band ferromagnetism in $SrRuO_3$ from neutron diffraction, J. Magn. Magn. Mat. **305**, 491 (2006).

[20] S. Lee, J.R. Zhang, S. Torii, S. Choi, D.-Y. Cho, T. Kamiyama, J. Yu, K.A. McEwen, and J.-G. Park, Large in-plane deformation of RuO_6 octahedron and ferromagnetism of bulk $SrRuO_3$, J. Phys. Condens. Matter **25**, 465601 (2013).

[21] Š. Masys and V. Jonauskas, A first-principles study of structural and elastic properties of bulk $SrRuO_3$, J. Chem. Phys. **139**, 224705 (2013).

[22] K. Momma and F. Izumi, *VESTA 3* for three-dimensional visualization of crystal, volumetric and morphology data, J. Appl. Crystallogr. **44**, 1272 (2011).

KRISTALINĖ $SrRuO_3$ SANDARA: HIBRIDINIO METODO TAIKYMAS KIETŲJŲ KŪNŲ TANKIO FUNKCIONALAMS

Š. Masys, V. Jonauskas

Vilniaus universiteto Teorinės fizikos ir astronomijos institutas, Vilnius, Lietuva

Santrauka

$SrRuO_3$ – perovskitinis kristalas, vertinamas dėl savo laidumo ir feromagnetinių savybių, taip pat labai gero struktūrinio suderinamumo su įvairiais funkciniais oksidais, naudojamais auginant perspektyvias heterosandūras ir supergardeles. Įprastinėmis sąlygomis $SrRuO_3$ pasižymi ortorombine kristaline sandara, tačiau visai neseniai tyrėjams pavyko stabilizuoti tetragonines bei monoklinines šios medžiagos fazes, kurioms dar reikia išsamesnių tyrimų. Norint atkartoti ir išanalizuoti pasiektus rezultatus teoriniu lygmeniu, būtina identifikuoti patikimas teorines priemones, užtikrinančias kuo didesnį tikslumą. Todėl šiame darbe taikome hibridinį tankio funkcionalo teorijos metodą kietųjų kūnų tyrimams, pritaikytiems apibendrintiesiems gradientiniams artiniams, bandydami sistemiškai nustatyti optimalią Hartrio ir Foko (HF) pakaitinės energijos dalį, leidžiančią tiksliausiai atkurti ortorombinės $SrRuO_3$ fazės kristalinę sandarą. Nustačius optimaliausią HF pakaitinės energijos indėlį, galima tikėtis, kad tokia HF ir tankio funkcionalų kombinacija bus veiksminga ir kitų dar netyrinėtų $SrRuO_3$ fazių atžvilgiu, todėl ją bus galima rekomenduoti ateities tyrimams. Taip pat pateikiame konkretų taikymo pavyzdį, kai geometrijos optimizacija, atlikta plonųjų $SrRuO_3$ plėvelių sistemai, leidžia tiksliai identifikuoti jos erdvinę grupę.